Journal of Power Sources 306 (2016) 636–645

Contents lists available at ScienceDirect

Journal of Power Sources

journal homepage: www.elsevier.com/locate/jpowsour

A fractal time thermal model for predicting the surface temperature of air-cooled cylindrical Li-ion cells based on experimental measurements

Jorge Reyes-Marambio [a], Francisco Moser [b], Felipe Gana [a], Bernardo Severino [a], Williams R. Calderón-Muñoz [a, b, *], Rodrigo Palma-Behnke [a, c], Pablo A. Estevez [a, c], Marcos Orchard [a, c], Marcelo Cortés [a, d]

[a] Energy Center, Universidad de Chile, Tupper 2007, Santiago, Chile
[b] Department of Mechanical Engineering, Universidad de Chile, Beauchef 851, Santiago, Chile
[c] Department of Electrical Engineering, Universidad de Chile, Tupper 2007, Santiago, Chile
[d] Department of Electrical Engineering, Universidad de Antofagasta, Av. Angamos 601, Antofagasta, Chile

HIGHLIGHTS

- A fractal time temperature model for cylindrical Li-ion cells is proposed.
- A spatially isolated single cell and two arrays of cells were experimentally studied.
- Cell surface temperature measurements were obtained at 1 C discharge rate.
- Stretched models show better agreement with experimental data than pure exponentials.
- The proposed fractal models predict thermal response and heat generation of cells.

ARTICLE INFO

Article history:
Received 11 August 2015
Received in revised form
3 November 2015
Accepted 12 December 2015
Available online 28 December 2015

Keywords:
Fractal time models
Stretched exponential models
Experimental thermal response
Lithium-ion cell heat generation

ABSTRACT

This paper presents a experimentally-validated fractal time thermal model to describe the discharge and cooling down processes of air-cooled cylindrical Lithium-ion cells. Three cases were studied, a spatially isolated single cell under natural convection and two spatial configurations of modules with forced air cooling: staggered and aligned arrays with 30 and 25 cells respectively. Surface temperature measurements for discharge processes were obtained in a single cell at 1 C, 2 C and 3 C discharge rates, and in the two arrays at 1 C discharge rate. In the modules, surface temperature measurements were obtained for selected cells at specific inlet cooling air speeds. The fractal time energy equation captures the anomalous temperature relaxation and describes the cell surface temperature using a stretched exponential model. Stretched exponential temperature models of cell surface temperature show a better agreement with experimental measurements than pure exponential temperature models. Cells closer to the horizontal side walls have a better heat dissipation than the cells along the centerline of the module. The high prediction capabilities of the fractal time energy equation are useful in new design approaches of thermal control strategies of modules and packs, and to develop more efficient signal-correction algorithms in multipoint temperature measurement technologies in Li-ion batteries.

1. Introduction

Energy storage is a technological problem for a wide range of applications. Many types of energy storage devices (ESD) have been developed in the past, including water dams for hydraulic turbines, heat storage for solar energy conversion systems, electric energy for electromobility and stationary storage systems. Currently, batteries are the main component in most electric storage systems.

The cells with higher energy densities are based on Lithium-ion technology, where modules and packs are designed to satisfy high

* Corresponding author. Department of Mechanical Engineering, Universidad de Chile, Beauchef 851, Santiago, Chile. Tel.: 56 229784469; fax: 56 226988453.
E-mail address: wicalder@gmail.com (W.R. Calderón-Muñoz).

http://dx.doi.org/10.1016/j.jpowsour.2015.12.037
0378-7753/

standards in safety and electrical requirements. Most of the applications for batteries in electromobility and energy storage for grid stabilization require high capacities and levels of power [1,2].

A wide set of chemical reactions are involved in charge and discharge processes of Lithium-ion batteries [3]. These reactions produce thermal processes that can release or absorb heat, yielding non-uniform temperature distributions in cells, modules, and packs [4]. Temperature differences among cells within modules and battery packs greatly affect the electrical performance of cells, reducing the expected lifetime of each module and consequently, of the whole battery [5]. This problem needs to be addressed with better cells and a well designed thermal system [6,7]. The main purpose of the cooling systems typically installed on battery packs is to remove temperature hot spots and keep the average temperature of modules between 25 $^{\circ}C$ and 40 $^{\circ}C$, as well as a maximum cell to cell temperature difference of 5 $^{\circ}C$. This allows us to achieve a good balance between performance and lifetime [8], as well as to prevent catastrophic accidents due to thermal runaways [9]. One of the most commonly used cooling systems in battery packs is forced air flow, mainly due to its simplicity in terms of equipment and low cost. This allows dissipating heat and keeping maximum temperature of the cells under control. However, it is necessary to design a strong forced air cooling system to minimize cell-to-cell temperature differences. An strategy to obtain an uniform temperature is to use distributed air flow [10].

The thermal control of a battery module would be easier if a mathematical model were known. System identification is very crucial in a thermal system with convection because the heat transfer coefficient is difficult to estimate with precision and may vary over time due to spatial configuration of cells and physical or chemical changes at the cell surface. Other heat transfer coefficients, such as heat capacity and thermal diffusivity of cells, also have to be determined. Instead of finding each coefficient separately, it seems more convenient to estimate a combined group that best fits experimental data. A lumped-parameter energy balance in which the temperature of the system is assumed to be spatially uniform is commonly used to model transient conductive systems exposed to convective heat fluxes at their boundaries [11]. When the heat convection away from the cell surface is faster than the heat conduction inside of it, there is a difference between the actual temperature field and the spatial average used in the lumped model. Non-integer order differential equations have been proposed as an approximate mathematical model, which can be readily fitted to temperature measurements and can be used to back out the heat transfer coefficients in real time at a low computational cost [12]. Examples of non-integer order differential equations are fractal derivatives, which have been applied to problems in physics and engineering, such as turbulence and anomalous diffusion [13–15].

Some recent studies in thermal management of battery modules and packs have focused in the development of low computational cost parametric models. For example, Hu et al. [16] developed a Foster-Network model to represent the interaction among cells achieving a low error with respect to a computational fluid dynamics (CFD) simulation. Park et al. [17] created a one-dimensional heat conduction model for a cell, coupled with a battery module model to predict the cell to cell temperature variation and power consumption. They found that a wide battery module with a small cell to cell gap is desirable for the air type battery thermal management system (BTMS), while a narrow battery module with a small gap is desirable for liquid type BTMS. Mousavi et al. [18] used genetic algorithms to find an optimal thermal management of a Lithium-ion battery. Fast design process and optimal design algorithms of battery modules and packs can benefit from the use of low-cost computational models with accurate prediction capabilities [19].

Experimentally-validated thermal models have been developed for single cylindrical cells. For instance, Shah et al. [20] studied the temperature rises due to transient heat generation rates and the effect of thermal parameters on temperature distribution in the cell. Radial thermal conductivity and the axial convection heat transfer coefficient can contribute significantly to a temperature reduction of the cells [21]. Forgez et al. [22] developed an estimation method of the internal temperature based on the surface temperature of a cylindrical cell. Li et al. [23] found significant temperature non-uniformity and differences between experimental measurements and CFD simulations of surface temperature in a battery module of cylindrical cells.

Thermophysical properties of cylindrical cells have been obtained in the literature through experimental measurements. For example, Drake et al. [24] proposed a method to measure the axial and radial thermal conductivity and heat capacity of cylindrical cells. Murashko et al. [25] introduced a methodology to determine the thermal conductivity and heat capacity in a pouch cell using gradient heat flux sensors.

In this paper, we investigate the discharge and cooling down processes in terms of temperature and heat generation of a spatially isolated single cell under natural convection, as well as 30-cell and 25-cell modules with forced air cooling through physical experiments. Surface temperature measurements for single cells were at 1 C, 2 C and 3 C discharge rates, and for modules were at 1 C discharge rate. A novel fractal time energy balance equation is presented and the temperature in both processes is well described by stretched exponential models where the thermal time constant and the influence of the speed of cooling flow are considered, and as a consequence, a model for the heat generation of cells is obtained for the discharge process. A comparison between stretched exponential and pure exponential models in the cooling down process for the single cell case is also presented.

2. Review of fractal differential equations

Fractal differential equations are applied to model a variety of non-integer power law scaling phenomena such as turbulence, fractional quantum mechanics, and anomalous diffusion [13,14]. Fractal time models describe systems with highly intermittent self-similar temporal behavior that does not possess a characteristic time scale. The time scale exists when the average time of an event is finite. Therefore, for fractal time the average time of an event must be infinite. For instance, this event can be the time a fluid particle spends in a given vortex. The lack of an average time induces fractional exponents. More details and explanation about fractal time can be found in Ref. [26].

We employ the fractal derivative defined as follows in Eq. (1) [14],

$$\frac{dF^{\beta}}{dt^{\gamma}} = \lim_{\Delta t \to 0} \frac{F^{\beta}(t+\Delta t) - F^{\beta}(t)}{(\Delta t + t)^{\gamma} - t^{\gamma}}, \tag{1}$$

where $\beta > 0$ is scaling or stretching factor for the dependent variable F and $\gamma > 0$ is a scaling or stretching factor for the time t. For explanation purposes, we consider a fractal derivative anomalous diffusion equation as shown in Eq. (2),

$$\frac{dF^{\beta}}{dt^{\gamma}} = -F^{\beta}(t^{\gamma}). \tag{2}$$

The analytical solution of Eq. (2) is found to be in the form of a stretched Gaussian distribution defined as follows in Eq. (3) [14].

$$F(t) = \left(e^{-t^{\gamma}}\right)^{1/\beta}. \quad (3)$$

The physical idea of the fractal time model is that the anomalous relaxation is the consequence of the breakdown of the adiabatic approximation in strongly coupled systems, in other words, the relaxation is a quasi-stationary process. Under the adiabatic approximation, the relaxation is a continuous process in terms of time. This approximation fails at a limiting time scale in strongly coupled systems [27].

3. Physical experiments

Battery cells generate heat during charge and discharge processes due to chemical reactions. The operating conditions of a module in a battery pack are determined by the specific application. The electrical requirements can change abruptly in some cases, and the cooling system has to be able to dissipate heat quickly in order to secure the module and cells. Thermal management of electrical devices involves the design of cooling systems to achieve the required heat dissipation rates and temperatures. The thermal inertia of modules and packs depends on the cooling system. In terms of thermal control, a cooling strategy can be qualified according to its thermal time constant. Our goal is to measure the temperature of cells in the discharge and cooling down processes, and estimate the heat generation of a cell and the effects of cooling flow speed in two spatial configurations of the cells: aligned and staggered.

3.1. Experimental setup

The experimental case, shown in Fig. 1a, was constructed with acrylic for an easy visual inspection of the testing section. The cells were connected in series, as shown in Fig. 1b. The design of the experimental setup was based on the specifications shown in Table 1. The experimental layout consisted of a 30-cell aligned array, shown in Fig. 2a, and a 25-cell staggered array, shown in Fig. 2b. Each cell has a 4.2 Open Circuit Voltage (OCV), so the aligned and staggered arrays have 125 and 105 OCV, respectively. A different number of cells is used in each array to maintain the width and length of the experimental domain, and consequently, to put at the same location lateral and horizontal walls, and cooling air inlet and outlet sections in both arrays. The cooling air flow is obtained using two Embpaspt 4412 FNH DC fans. Each fan was connected to a 3 m tube to ensure the developed flow regime. Each pack was discharged and electrically monitored using a custom made Power Inverter. The temperature of the remarked cells was monitored using LM35DZ temperature sensors. These sensors were connected to a National Instrument 9201 module. The data from the sensors was obtained using a National Instruments CompactRio module, and processed with the National Instrument LabView 2013 software using an acquisition frequency of 1 s. The test set-up for experimental measurements is shown in Fig 2c.

3.2. Methods

The experiments were performed on a spatially isolated single cell under natural convection and two modules with forced air cooling at 1 C discharge currents. This discharge rate was chosen since according to the electric specifications of the cylindrical cells ICR-26650 being used, shown in Table 2, it is the nominal operating condition and there should not be any issue to perform the sensor and variability analysis by repeating the experiments with the same cells. When the cells in the modules reach the cut-off voltage

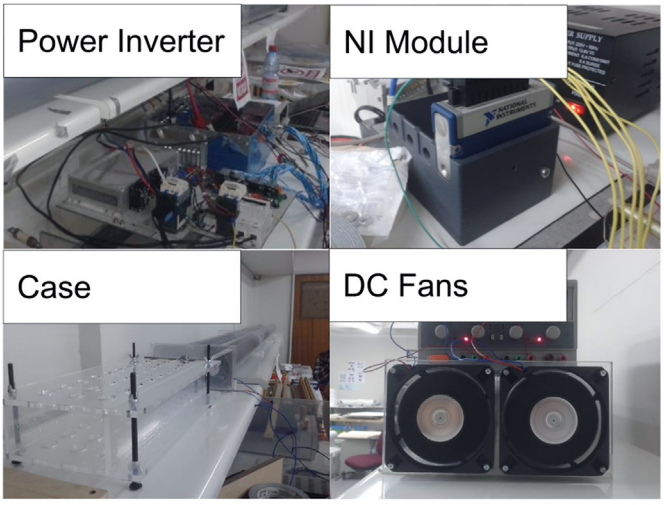

(a) Experimental components

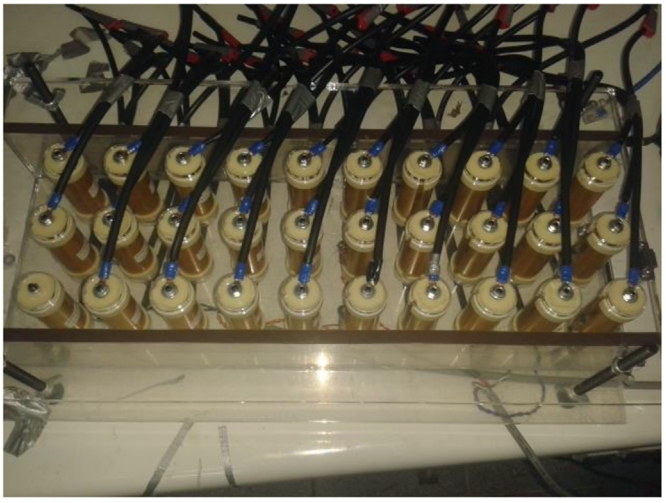

(b) Cells connected in series

Fig. 1. Experimental setup.

Table 1
Design of the experimental setup.

Monitoring	
Temperature sensor	LM335DZ
Data Adquisitor	NI 9201 Module
Software	LabView 2013
Electrical monitoring	Custom Inversor
Cooling Flow	
Dc Fans	Embpapst 4412FNH
Velocity inlet	0, 2.0, 2.5 ms^{-1}
Electrical Information	
Configuration	30 and 25 series cell
Discharge current	4 A

shown in Table 2, the DC fans were turned on. The temperature of the cells were monitored both in the discharge of the module and in the cooling down process. Due to technical limitations, experiments at 1 C, 2 C and 3 C discharge currents were performed on a A123 ANR26650 M1A spatially isolated single cell.

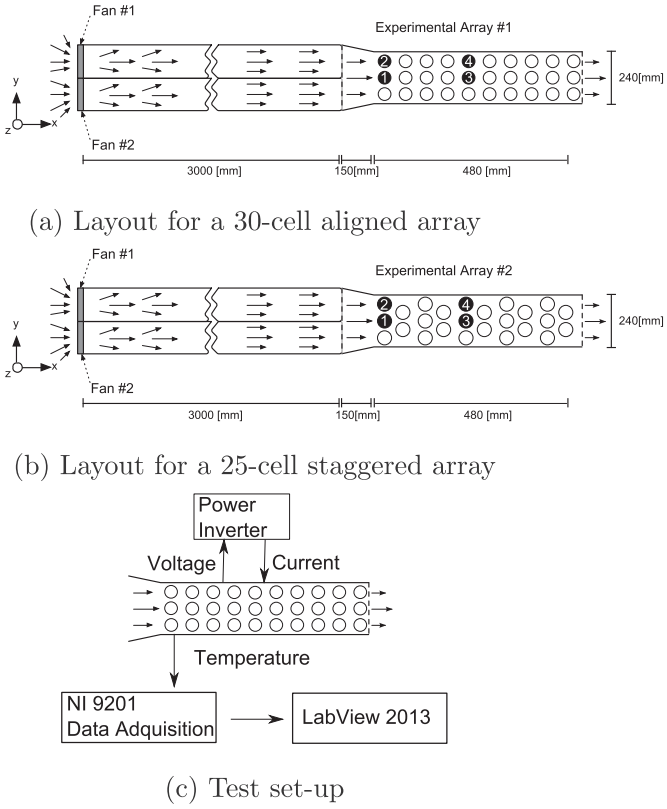

Fig. 2. Experimental layout and test set-up for experimental measure-ments.

Table 2
Specifications of cylindrical Lithium-ion cell (ICR-26650 manufactured by Battery Building Group).

Mechanical properties	
Diameter	26 mm
Height	65 mm
Mass	0.095 Kg
Heat capacity [24]	1650 JKg^{-1} K^{-1}
Electric Properties	
Nominal voltage	3.7 V
Cut off voltage	2.7 V
Nominal capacity @1 C at 20 °C	4.0 Ah
Initial internal resistance	26 mΩ
Maximum continuous current	4 A

3.2.1. Sensor and system variability analysis

A variability analysis was performed on a set of 10 experiments designed to measure surface temperature as a function of time in the cooling down process for a specific cell, whose specifications are shown in Table 2, in the aligned 30-cell module. The operating conditions were complete discharge at room temperature, then the cooling air velocity was set at 2.5 ms^{-1}. The average surface temperature as a function of time and standard deviation are shown in Fig. 3. In this figure $\overline{T}\pm\sigma$ indicates the average temperature obtained in 10 experiments plus or less 1 standard deviation. Since the standard deviation is small, the experimental setup and data acquisition equipment and setting can be considered able to satisfy a reasonable repeatability and reproducibility of the experiment.

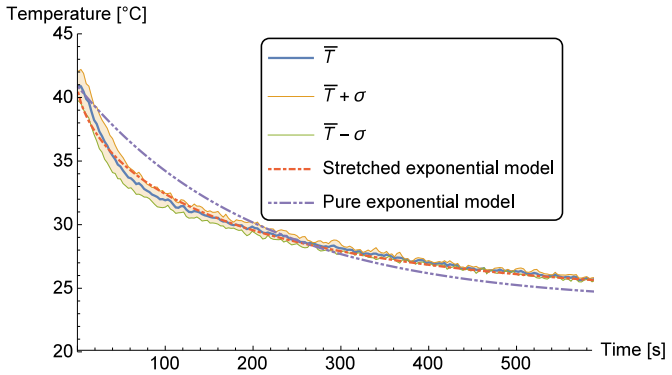

Fig. 3. Variability analysis based on surface temperature measurements for cooling down process of cell #1 in aligned module. $\overline{T}$ is the average sur-face cell temperature over time and _ is the standard deviation.

4. Mathematical modeling

4.1. General lumped-parameter energy balance equation

The general lumped-parameter energy balance equation for a single cell in a module is written as follows in Eq. (4),

$$\frac{dT}{dt} = -\frac{1}{\tau}(T(t) - T_\infty) + \frac{1}{\rho_c C_p V_c} Q_{gen}(t), \tag{4}$$

where $\tau = \rho_c C_p V_c / h_m A_c$ is the thermal time constant and T is the surface temperature of the cell, t is time, ρ_c is the density, C_p is the specific heat of the cell, V_c is the volume of the cell, A_c is the surface area of the cell, h_m is the convective heat transfer coefficient for a specific cell, T_∞ is the room temperature, and $Q_{gen}(t)$ is the heat generated inside the cell. The specific heat coefficient is weakly dependent on temperature [22,28], so the assumption of constant specific heat of the cell is well justified.

A mathematical model describing the cell temperature is useful to perform the thermal control of a battery module. A thermal model based on a lumped-parameter energy balance, as described in Eq. (4), is valid to predict cell surface temperature as a function of time in the cooling down process under the assumption that the cell temperature is spatially uniform. In terms of heat transfer, it means that heat conduction inside the cell is faster than the heat convection away from the cell surface, and there are no exothermic or endothermic processes inside the cell during the cooling down process.

4.2. Fractal time energy balance equation

We propose a fractal time energy balance equation to describe the surface temperature for a single cell in the battery module, as shown in Eq. (5),

$$\frac{dT^\alpha}{dt^\alpha} = -\frac{1}{\tau^\alpha}\left(T^\alpha(t^\alpha) - T_\infty^\alpha\right) + \frac{1}{\left(\rho_c C_p V_c\right)^\alpha} Q_{gen}^\alpha(t^\alpha). \tag{5}$$

The stretching parameter, α, represents a scaling factor of the temperature and the time in the model. A fractal differential equation model is a non-integer differential equation to model complex systems. Recently, non-integer differential equations have been used to model transient thermal systems with anomalous heat dissipation [12,14,15].

4.3. Cooling down process

4.3.1. Pure exponential model

A pure exponential model to describe the cell surface temperature as a function of time in the cooling down process is presented in Eq. (6)

$$T(t) = (T(0) - T_\infty)e^{-\left(\frac{t}{\tau}\right)} + T_\infty. \tag{6}$$

This model is the solution of the energy balance equation shown in Eq. (7), which corresponds to the general lumped-parameter energy balance equation for a single cell shown in Eq. (4) when $Q_{gen}(t) = 0$.

$$\frac{dT}{dt} = -\frac{1}{\tau}(T(t) - T_\infty). \tag{7}$$

4.3.2. Stretched exponential model

A stretched exponential model to describe the cell surface temperature as a function of time in the cooling down process is presented in Eq. (8)

$$T(t^\alpha) = \left[(T^\alpha(0) - T_\infty^\alpha)e^{-\left(\frac{t}{\tau}\right)^\alpha} + T_\infty^\alpha\right]^{1/\alpha}. \tag{8}$$

This model is the solution of the fractal time model shown in Eq. (9), which corresponds to the proposed energy balance equation for a single cell shown in Eq. (5) when $Q_{gen}^\alpha(t^\alpha) = 0$.

$$\frac{dT^\alpha}{dt^\alpha} = -\frac{1}{\tau^\alpha}(T^\alpha(t^\alpha) - T_\infty^\alpha). \tag{9}$$

Stretching exponential models have many applications in modeling numerous types of experimental relaxation data in complex systems with *anomalous relaxation*. Examples of temporal scaling laws involving non-integer exponents include dielectric relaxation, nuclear magnetic relaxation, and stress-relaxation [26,29,30].

From the variability analysis in the cooling down process shown in Fig. 3, it is obtained that the stretched exponential model provides a better fitting to experimental measurements than the pure exponential model. Due to this, the stretched exponential model can be used to identify in real time and at a low computational cost convection heat transfer coefficients in the group τ that best fits experimental data. The differences between the predicted temperatures from stretched and pure exponential models with respect to surface temperature measurements for a case of cooling down process are shown in Fig. 4. These temperature differences were used to obtain the prediction errors of the models. The percentage errors were calculated at every time as the ratio between the temperature differences and the surface temperature measurement. The stretched exponential model has a maximum error of 3.22% compared to average values from experimental data, on the other hand the pure exponential has a maximum error of 9.36%. Besides, the cumulative error for the stretched exponential model is 95.11° Celsius and for the pure exponential model is 378.11° Celsius.

4.4. Discharge process

For the spatially isolated cell, natural convection is taking out the cell heat not only in the cooling down process, but also in the discharge process. On the other hand, the discharge process for each cell in the modules is under natural convection conditions since the forced cooling is only used in the cooling down process. A model of the cooling down process allows us to estimate the heat dissipation under the specific configuration and operating conditions. This heat dissipation from the cells is useful to determine the heat generation term in the general lumped-parameter energy balance equation for a single cell as described in Eq. (4) with a thermal time constant, τ_0, using a natural convection heat transfer coefficient.

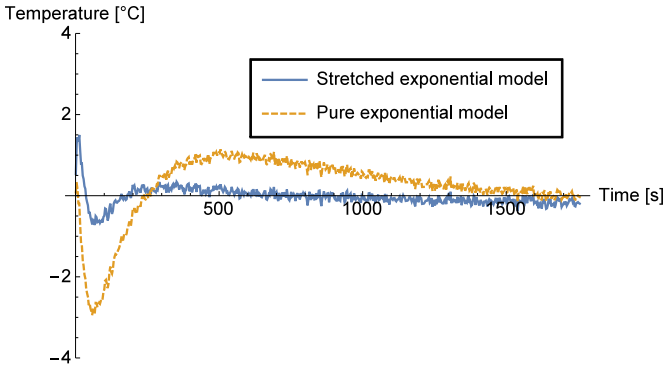

Fig. 4. Temperature differences between stretched and pure exponential models with respect to surface temperature measurements for cooling down process of cell #1 in aligned module.

Since natural convection is taking out the cell heat and due to experimental results shown in Figs. 3 and 4, we also proposed a fractal time model as energy balance equation to describe the surface temperature in the discharge process for a single cell in the battery module, as shown in Eq. (5).

4.5. Empirical surface temperature model in discharge process

The solution of Eq. (4) and Eq. (5) to predict the cell surface temperature depends on the heat generation of the cell, $Q_{gen}(t)$. In order to estimate the heat generation in both the general lumped-parameter and fractal time models, we propose a fitting model to surface temperature measurements in discharge process, as described in Eq. (10),

$$T(t^\alpha) = \left[Ce^{a\left(\frac{t}{\mu}\right)^\alpha} tanh\left(b\left(\frac{t}{\mu}\right)^\alpha\right) + T^\alpha(0)\right]^{1/\alpha}, \tag{10}$$

where a, b and C are constants and μ is the discharge time. This temperature model for the discharge process, the stretched exponential model for the cooling down process and experimental measurements for the spatially isolated cell are shown in Fig. 5a.

4.6. Heat generation model

For comparison purposes, the cell heat generation is obtained using the general energy equation and the fractal time energy equation for the discharge process, Eq. (4) and Eq. (5), respectively. Model parameters and thermal coefficients have to be known in order to obtain the cell heat generation.

The heat generation using the general lumped-parameter model is:

$$Q_{gen}(t) = \rho_c C_p V_c\left[\frac{dT}{dt} + \frac{1}{\tau_0}(T(t) - T_\infty)\right]. \tag{11}$$

The heat generation using the fractal time model is:

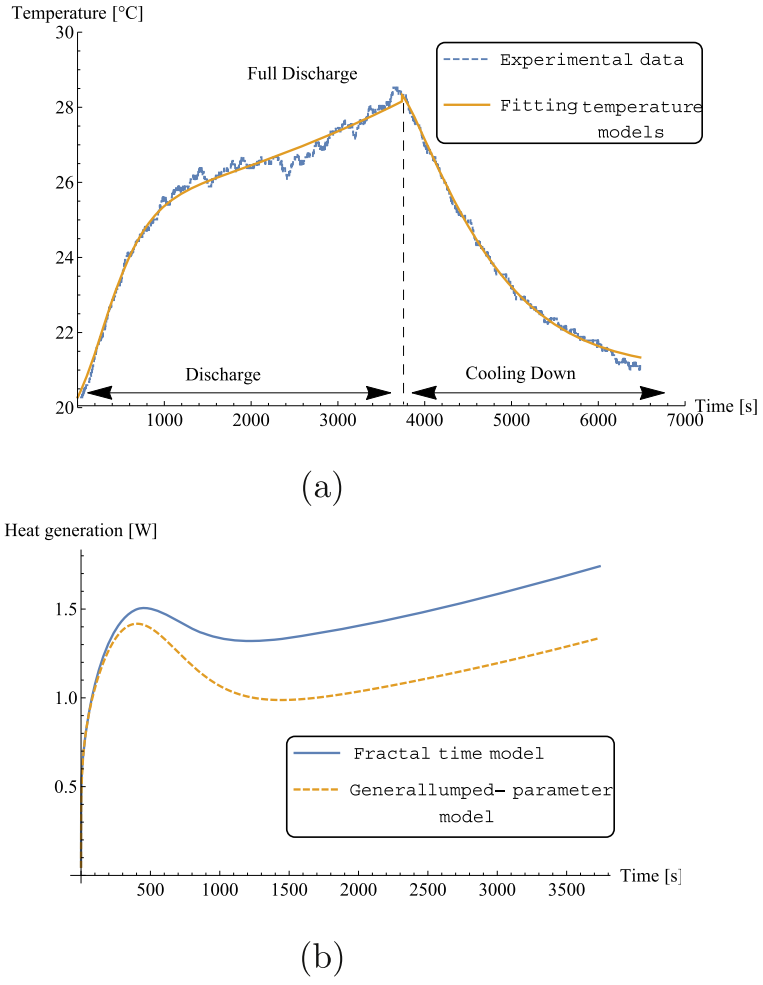

Fig. 5. Spatially isolated single cell under natural convection at 1 C discharge rate. a) Surface temperature as a function of time and fitting of discharge process and stretched exponential models to experimental data with $\alpha = 1.21$ and $\tau = 1070.55$. b) Heat generation rate.

$$Q_{gen}(t^{\alpha}) = \rho_c C_p V_c \left[\frac{dT^{\alpha}}{dt^{\alpha}} + \frac{1}{\tau_0^{\alpha}} \left(T^{\alpha}(t^{\alpha}) - T_{\infty}^{\alpha} \right) \right]^{1/\alpha}. \tag{12}$$

5. Results and discussion

5.1. Fitting models to experimental data

5.1.1. Surface temperature of spatially isolated single cell under natural convection

Surface temperature measurements made in a single cylindrical cell under specifications shown in Table 2, were performed in a discharge process at 1 C and in the cooling down process without forced air cooling. Temperature reaches a maximum value at full electrical discharge, as shown in Fig. 5a. The cooling down process is governed by natural convection heat transfer from the cell surface at room temperature.

Table 3
Specifications of cylindrical Lithium-ion cell (A123 ANR26650 M1A).

Mechanical properties	
Diameter	26 mm
Height	65 mm
Electric Properties	
Nominal voltage	3.3 V
Cut off voltage	2.0 V
Nominal capacity @1 C at 20 °C	2.3 Ah
Maximum continuous current	70 A

5.1.2. Heat generation rate of spatially isolated single cell under natural convection

Temperature measurements of a spatially isolated single cell were used to estimate the heat generation shown in Fig. 5b. The pure exponential and the stretched exponential surface temperature models were used to obtain the heat generation rate. The predicted heat generation rate using the pure exponential model shows that there is a peak in the first half of the discharge process and a valley in the second half, while at the end of the discharge process the heat generation rate tends to increase. Using the stretched exponential model, the heat generation rate increases approximately at 0.0065 Ws^{-1} during the first 500 s, after this the heat generation rate increases slower approximately at 0.00016 Ws^{-1}. The predicted heat generation rate using the stretched exponential is always higher than the one predicted using the pure exponential model. Well-established heat generation models take into account internal electric resistance (Joule heating) and entropy changes [31]. The proposed model does not consider the Joule heating and entropy changes explicitly. However, the

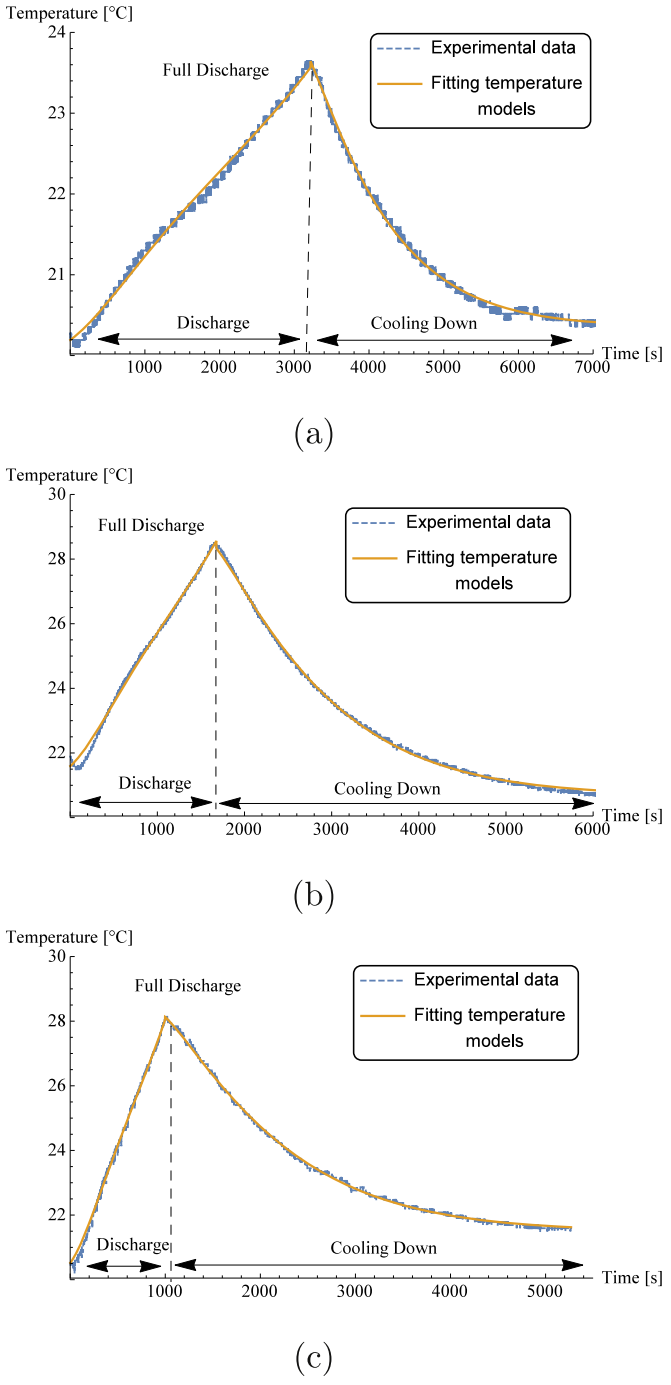

Fig. 6. Surface temperature as a function of time and fitting of dis-charge process and stretched exponential models to experimental data in a spatially isolated A123 cell under natural convection at higher discharge rates. a) 1 C discharge current, $\alpha = 1.12$ and $\tau = 1095.21$. b) 2 C discharge current, $\alpha = 1.15$ and $\tau = 1344.11$. c) 3 C discharge current, $\alpha = 1.17$ and 1 $\tau = 1315.77$.

predicted heat generation from Eq. (12) is in agreement with the trend of heat generation rates during constant current discharges as recently reported [32].

5.1.3. Surface temperature of spatially isolated single cell under natural convection at higher discharge rates

The manufacturer of the cylindrical cells specified in Table 2 do not recommend to operate the cells at higher discharge rates than 1 C. Due to this and the fact that we are not performing destructive tests, we select to use a cylindrical A123 ANR26650 M1A cell under specifications shown in Table 3, at 1 C, 2 C and 3 C discharge currents and measuring surface temperature as shown in Fig. 6. We found that the stretched exponential model provides a better fitting of the cell surface temperature as a function of time in the cooling down process than the pure exponential model.

5.1.4. Modules with forced air cooling

Measurements show similar surface temperature values between cells 1 and 2, and between cells 3 and 4, in both, aligned and staggered configurations. Due to this, only temperature measurements for cells 1 and 3 are considered for analysis and discussion in this study. Examples of temperature measurements for the aligned configuration with forced air speeds of 2.5 ms^{-1} and 2.0 ms^{-1} are shown in Fig. 7. These measurements allow us to determine the changes in the model parameters due to variations in the heat dissipation rates. These particular values of forced air speeds were chosen to satisfy the requirement of developed flow regime in the inlet of the testing section, taking into account the length and diameter of tubes (120 mm) between the fans and testing section, and also fans technical specifications. In order to obtain these forced air speeds, the fans are set at 100% and 80% of their nominal electrical power. Model fitting results show that α and the thermal time constant τ increases with a lower cooling air flow speed in the air flow direction. For the staggered configuration, examples of temperature measurements with forced air speeds of 2.5 ms^{-1} and 2.0 ms^{-1} are shown in Fig. 8. Model fitting results show that α

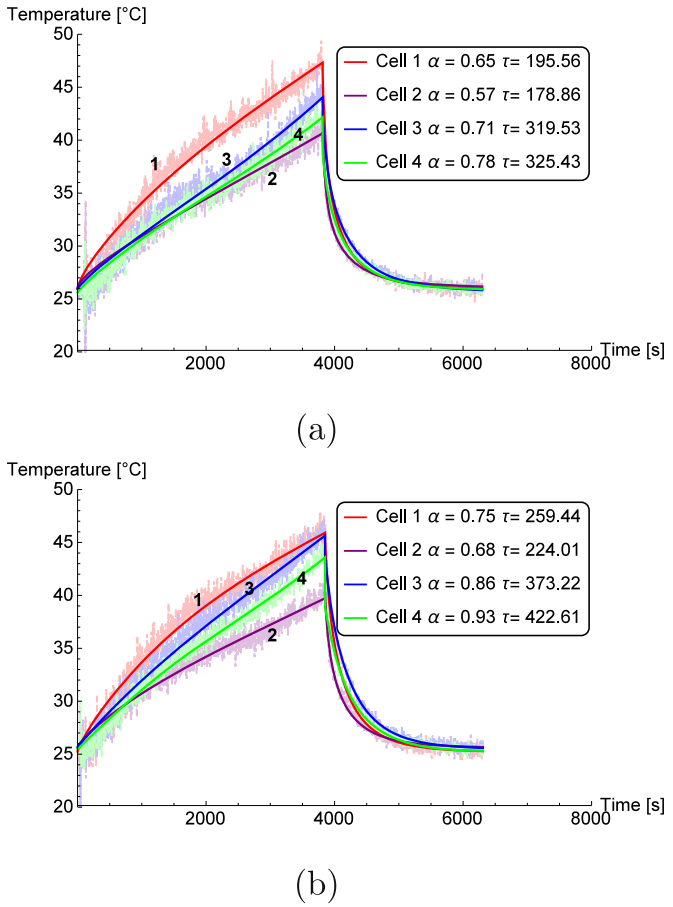

Fig. 7. Experimental measurements of surface temperature in aligned array. Continuous line represents the fitting of stretched exponential model. a) Cooling air flow speed at 2.5 ms^{-1}. b) Cooling air flow speed at 2.0 ms^{-1}.

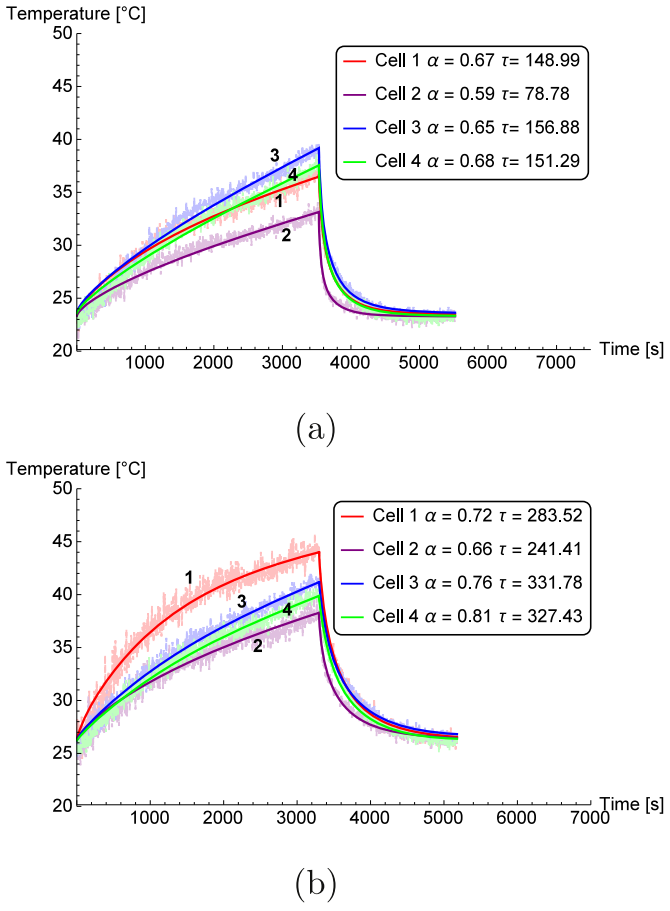

Fig. 8. Experimental measurements of surface temperature in staggered array. Continuous line represents the fitting of stretched exponential model. a) Cooling air flow speed at 2.5 ms^{-1}. b) Cooling air flow speed at 2.0 ms^{-1}.

decreases slightly as the cooling air is reduced, and takes higher values for cells located downstream in the module. On the other hand, τ increases strongly as the cooling air flow is reduced, and also takes higher values for cells located downstream in the module, where the increase is substantially higher in the staggered case than in the aligned case. This could be due to the pressure drop of the cooling air flowing through the cells in the testing section. Experimental measurements need to be done in the near future to determine the behavior of τ and α at lower forced air speeds. The model parameters were obtained using non-linear fitting in the software Wolfram Mathematica with a confidence level of 0.95. The estimate values, standard errors (SE) and confidence intervals (CIs) of τ, α, a, b and C are shown for the aligned and staggered arrays in Tables 4 and 5, respectively.

5.2. Thermal effects and stretching parameter

In order to describe the discharge and cooling down processes in terms of surface temperature and heat generation, a spatially isolated single cell under natural convection, as well as 30-cell and 25-cell modules with forced air cooling at two speeds were studied. Variations in the stretching parameter, α, play a major role in variations of the thermal time constant, τ. In the model, α takes into account the temporal variations of heat transfer coefficients, such as convection and heat capacity, as well as spatial configurations of cells. The results show that α increases in the air flow direction and τ is lower for those cells closer to the horizontal side walls of the module. This indicates that the horizontal side walls of the module contribute to the heat dissipation. A pure exponential model requires $\alpha = 1$, under *anomalous relaxation* $\alpha \neq 1$. *Anomalous relaxation* in the cell cooling process is a relaxation with an intrinsic time, t^{α}, that takes into account an intermittent process instead of a continuous process [26]. A normal relaxation is a continuous process which can be modeled with a pure exponential model. Results show that $0 < \alpha < 1$ in the modules with forced air cooling and $\alpha > 1$ for the cells under natural convection.

Table 4
Fractal model parameters for aligned arrays. SE: Standard deviation, CI: Confidence interval.

Cell 1, 2.5 ms^{-1}			
	Estimate	SE	CI
α	0.65	0.01	0.64–0.66
τ	195.56	1.15	192.61–198.52
a	0.70	0.24	0.23–1.16
b	1.49	0.43	0.63–2.34
C	2.19	0.71	0.80–3.57
Cell 2, 2.5 ms^{-1}			
	Estimate	SE	CI
α	0.57	0.01	0.640–0.660
τ	178.86	1.47	175.06–182.66
a	1.13	0.39	0.13–2.13
b	1.43	0.70	−0.37–3.23
C	0.67	0.36	−0.27–1.60
Cell 3, 2.5 ms^{-1}			
	Estimate	SE	CI
α	0.71	0.01	0.70–0.72
τ	319.53	1.63	315.33–323.73
a	1.41	0.07	1.27–1.55
a	2.26	0.19	1.88–2.64
C	1.16	0.09	0.99–1.34
Cell 4, 2.5 ms^{-1}			
	Estimate	SE	CI
α	0.78	0.01	0.76–0.79
τ	325.43	2.60	318.73–332.14
a	1.25	0.05	1.12–1.38
b	2.46	0.14	2.09–2.83
C	1.70	0.08	1.48–1.92
Cell 1, 2.0 ms^{-1}			
	Estimate	SE	CI
α	0.75	0.01	0.74–0.76
τ	259.44	1.14	256.49–262.39
a	0.55	0.10	0.36–0.74
b	1.80	0.20	1.41–2.20
C	3.90	0.45	3.01–4.79
Cell 2, 2.0 ms^{-1}			
	Estimate	SE	CI
α	0.68	0.01	0.67–0.70
τ	224.01	1.55	220.01–228.01
a	0.93	0.11	0.64–1.23
b	1.89	0.25	1.25–2.53
C	1.32	0.17	0.87–1.77
Cell 3, 2.0 ms^{-1}			
	Estimate	SE	CI
α	0.86	0.01	0.84–0.87
τ	373.22	1.68	368.89–377.55
a	0.89	0.07	0.76–1.02
b	2.08	0.15	1.78–2.37
C	4.33	0.31	3.73–4.93
Cell 4, 2.0 ms^{-1}			
	Estimate	SE	CI
α	0.93	0.01	0.90–0.95
τ	422.61	3.30	414.09–431.13
a	1.04	0.03	0.96–1.11
b	2.73	0.09	2.49–2.98
C	4.63	0.13	4.30–4.97

5.3. Improvements in designing battery modules

The thermal behavior of the cells in a module can be improved

Table 5
Fractal model parameters for staggered array. SE: Standard deviation, CI: Confidence interval.

Cell 1, 2.5 ms^{-1}			
	Estimate	SE	CI
α	0.67	0.01	0.65–0.68
τ	148.99	1.42	145.33–152.66
a	0.62	0.11	0.41–0.83
b	1.76	0.21	1.34–2.17
C	1.59	0.20	1.19–1.99
Cell 2, 2.5 ms^{-1}			
	Estimate	SE	CI
α	0.59	0.01	0.56–0.61
τ	78.78	1.57	74.71–82.85
a	0.80	0.33	−0.04–1.64
b	1.42	0.58	−0.08–2.92
C	0.73	0.33	−0.13–1.60
Cell 3, 2.5 ms^{-1}			
	Estimate	SE	CI
α	0.65	0.01	0.64–0.66
τ	156.88	1.28	153.58–160.18
a	0.76	0.23	0.32–1.20
b	1.45	0.49	0.66–2.24
C	1.60	0.50	0.63–2.58
Cell 4, 2.5 ms^{-1}			
	Estimate	SE	CI
α	0.68	0.01	0.66–0.69
τ	151.30	1.46	147.53–155.06
a	0.79	0.21	0.24–1.33
b	1.47	0.38	0.49–2.46
C	1.58	0.45	0.41–2.75
Cell 1, 2.0 ms^{-1}			
	Estimate	SE	CI
α	0.72	0.01	0.71–0.73
τ	283.52	1.70	279.12–287.92
a	0.22	0.01	0.03–0.41
b	1.77	0.19	1.39–2.15
C	4.03	0.47	3.11–4.96
Cell 2, 2.0 ms^{-1}			
	Estimate	SE	CI
α	0.66	0.01	0.65–0.68
τ	241.41	2.24	235.61–247.20
a	0.57	0.31	−0.24–1.38
b	1.47	0.57	0.01–2.93
C	1.58	0.68	−0.16–3.33
Cell 3, 2.0 ms^{-1}			
	Estimate	SE	CI
α	0.76	0.01	0.75–0.78
τ	331.77	1.95	326.75–336.80
a	0.57	0.11	0.35–0.78
b	1.67	0.21	1.26–2.08
C	3.03	0.41	2.23–3.83
Cell 4, 2.0 ms^{-1}			
	Estimate	SE	CI
α	0.81	0.01	0.80–0.83
τ	327.43	1.99	322.28–332.58
a	0.62	0.08	0.42–0.82
b	1.89	0.16	1.48–2.31
C	3.29	0.29	2.55–4.03

by reducing the number of cells facing at the same time the cooling air flow. For a specific number of cells, a spatial configuration where the side walls of the module in the air flow direction is larger than the side facing the cooling air flow improves the cooling of the cells, taking advantage of the interaction with the side walls.

6. Conclusions

Thermal behavior of a Li-ion cell in a module due to the interaction with upstream cells and operating conditions is important in practical applications for energy storage and conversion. We obtained a stretched exponential model based on experimental measurements of discharge and cooling down that predicts satisfactorily the surface temperature as a function of time in cylindrical Li-ion cells within a module, showing a better agreement with experimental measurements than pure exponential models. These stretched exponential models can be easily extended to more cells in the module, and may be used in developing a complete thermal model for a battery pack. Results were also confirmed for a single cell at higher discharge rates. The proposed models predict the thermal response and heat generation of cells in a module at low computational cost and with low error, becoming an efficient tool in new thermal control strategies and in quick explorations in optimization algorithms of suitable and novel Lithium-ion battery modules and packs design. Additionally, we think that these models could be used in new signal-correction algorithms in multipoint temperature measurement technologies, where detailed temperature measurements with high spatial resolution and envisioned temperature changes in modules and packs are required.

Future work should investigate other possible effects of the operating conditions which could change the stretching parameter of the fractal time model and the constants a,b and C. These include the effects of different C rates, forced air speeds and cell arrays. Lastly, it is advisable to study the applicability of the stretched exponential and fractal time models to different kind of Li-ion cells, such as prismatic and pouch.

Acknowledgments

We appreciate the helpful collaboration of Mr. Ignacio Polanco for some technical support. We are grateful to CORFO-Chile (11IDL1-10466 and 12IDL2-16296), CONICYT/ FONDAP (15110019) and Fondecyt 1151438 for their support.

References

[1] A. Thielmann, A. Sauer, R. Isenmann, M. Wietschel, P. Pltz, Product Roadmap Lithium-ion Batteries 2030, Technical Report, Fraunhofer Institute for Systems and Innovation Research ISI, 2012.
[2] J. Leadbetter, L.G. Swan, Selection of battery technology to support grid-integrated renewable electricity, J. Power Sources 216 (2012) 376–386.
[3] K. Smith, C.-Y. Wang, Power and thermal characterization of a lithium-ion battery pack for hybrid-electric vehicles, J. Power Sources 160 (2006) 662–673.
[4] S. Schoeffert, Thermal batteries modeling, self-discharge and self-heating, J. Power Sources 142 (2005) 361–369.
[5] Y. Ye, Y. Shi, N. Cai, J. Lee, X. He, Electro-thermal modeling and experimental validation for lithium ion battery, J. Power Sources 199 (2012) 227–238.
[6] A.A. Pesaran, G.-H. Kim, M. Keyser, Integration issues of plug-in and hybrid electric vehicles, in: EVS-24 International Battery, Hybrid and Fuel Cell Electric Vehicle Symposium, 2009.
[7] T.M. Bandhauer, S. Garimella, T.F. Fuller, A critical review of thermal issues in lithium-ion batteries, J. Electrochem. Soc. 158 (2011) R1–R25.
[8] A.A. Pesaran, Battery thermal models for hybrid vehicle simulations, J. Power Sources 110 (2002) 377–382.
[9] Q. Wang, P. Ping, X. Zhao, G. Chu, J. Sun, C. Chen, Thermal runaway caused fire and explosion of lithium ion battery, J. Power Sources 208 (2012) 210–224.
[10] G. Karimi, X. Li, Thermal management of lithium-ion batteries for electric vehicles, Int. J. Energy Res. 37 (2013) 13–24.
[11] F.P. Incropera, D.P. DeWitt, Fundamentals of Heat and Mass Transfer, fifth ed., John Wiley & Sons, New York, 2002.
[12] Y. Aoki, M. Sen, S. Paolucci, Approximation of transient temperatures in complex geometries using fractional derivatives, Heat Mass Transf. 44 (2008) 771–777.
[13] W. Chen, Time-space fabric underlying anomalous diffusion, Chaos Solit. Fractals 28 (2006) 923–929.
[14] W. Chen, H. Sun, X. Zhang, D. Korošak, Anomalous diffusion modeling by fractal and fractional derivatives, Comput. Math. Appl. 59 (2010) 1754–1758.
[15] W. Chen, L. Ye, H. Sun, Fractional diffusion equations by the Kansa method, Comput. Math. Appl. 59 (2010) 1614–1620.
[16] X. Hu, S. Lin, S. Stanton, W. Lian, A Foster network thermal model for HEV/EB battery modeling, Ind. Appl. IEEE Trans. 47 (2011) 1692–1699.
[17] S. Park, D. Jung, Battery cell arrangement and heat transfer fluid effects on the parasitic power consumption and the cell temperature distribution in a hybrid electric vehicle, J. Power Sources 227 (2013) 191–198.
[18] M. Mousavi, S. Hoque, S. Rahnamayan, I. Dincer, G. Naterer, Optimal design of

an air-cooling system for a li-ion battery pack in electric vehicles with a genetic algorithm, IEEE Congress on, in: Evolutionary Computation (CEC), 2011, pp. 1848–1855.
[19] B. Severino, F. Gana, R. Palma-Behnke, P.A. Estévez, W.R. Calderón-Muñoz, M.E. Orchard, J. Reyes, M. Cortés, Multi-objective optimal design of lithium-ion battery packs based on evolutionary algorithms, J. Power Sources 267 (2014) 288–299.
[20] K. Shah, S.J. Drake, D.A. Wetz, J.K. Ostanek, S.P. Miller, J.M. Heinzel, A. Jain, An experimentally validated transient thermal model for cylindrical Li-ion cells, J. Power Sources 271 (2014) 262–268.
[21] K. Shah, S.J. Drake, D.A. Wetz, J.K. Ostanek, S.P. Miller, J.M. Heinzel, A. Jain, Modeling of steady-state convective cooling of cylindrical Li-ion cells, J. Power Sources 258 (2014) 374–381.
[22] C. Forgez, D.V. Do, G. Friedrich, M. Morcrette, C. Delacourt, Thermal modeling of a cylindrical $LiFePO_4$/graphite lithium-ion battery, J. Power Sources 195 (2010) 2961–2968.
[23] X. Li, F. He, L. Ma, Thermal management of cylindrical batteries investigated using wind tunnel testing and computational fluid dynamics simulation, J. Power Sources 238 (2013) 395–402.
[24] S.J. Drake, D.A. Wetz, J.K. Ostanek, S.P. Miller, J.M. Heinzel, A. Jain, Measurement of anisotropic thermophysical properties of cylindrical Li-ion cells, J. Power Sources 252 (2014) 298–304.
[25] K.A. Murashko, A.V. Mityakov, J. Pyrhönen, V.Y. Mityakov, S.S. Sapozhnikov, Thermal parameters determination of battery cells by local heat flux measurements, J. Power Sources 271 (2014) 48–54.
[26] M.F. Shlesinger, Fractal time in condensed matter, Annu. Rev. Phys. Chem. 39 (1988) 269–290.
[27] C. Hong, W. Xiang, F. Jun-xin, Relaxation in condensed matter: a fractal time model, J. Phys. C Solid State Phys. 19 (1986) L499–L503.
[28] K. Onda, T. Ohshima, M. Nakayama, K. Fukuda, T. Araki, Thermal behavior of small lithium-ion battery during rapid charge and discharge cycles, J. Power Sources 158 (2006) 535542.
[29] J.C. Phillips, Stretched exponential relaxation in molecular and electronic glasses, Rep. Prog. Phys. 59 (1996) 1133–1207.
[30] R.K. June, J.P. Cunningham, D.P. Fyhrie, A Novel method for curvefitting the stretched exponential function to experimental data, Biomed. Eng. Res. 4 (2013) 153–158.
[31] A. Mills, S. Al-Hallaj, Simulation of passive thermal management system for lithium-ion battery packs, J. Power Sources 141 (2005) 307–315.
[32] S.J. Drake, M. Martin, D.A. Wetz, J.K. Ostanek, S.P. Miller, J.M. Heinzel, A. Jain, Heat generation rate measurement in a Li-ion cell at large C-rates through temperature and heat flux measurement, J. Power Sources 285 (2015) 266–273.